

## Two-photon entanglement of orbital angular momentum states

Sonja Franke-Arnold and Stephen M. Barnett

*Department of Physics and Applied Physics, University of Strathclyde, Glasgow G4 0NG, Scotland*

Miles J. Padgett and L. Allen

*Department of Physics and Astronomy, University of Glasgow, Glasgow G12 8QQ, Scotland*

(Received 12 January 2001; published 26 February 2002)

We investigate the orbital angular momentum correlation of a photon pair created in a spontaneous parametric down-conversion process. We show how the conservation of the orbital angular momentum in this process results from phase matching in the nonlinear crystal.

DOI: 10.1103/PhysRevA.65.033823

PACS number(s): 42.65.Ky, 42.50.Dv, 03.65.Ta

Entanglement is one of the most puzzling and powerful properties of quantum theory and has received undiminished attention since the earliest days of quantum mechanics. Entangled states play a crucial role in the investigation of the EPR paradox [1] and in the evaluation of Bell's inequality [2], which distinguishes between local and nonlocal formulations of quantum mechanics. However, two-photon entanglement not only poses fundamental questions to our understanding of quantum theory, but it also plays an important role in applications of quantum mechanics including quantum cryptography, teleportation [3,4], and quantum images [5–7].

Parametric down-conversion has proved a reliable tool for the generation of pairs of entangled photons [8,9]. The resulting spatially separated photons, usually named the “signal” and “idler,” are entangled in their arrival times at the respective detectors [10] and in their transverse positions [6]. They can also be entangled in their polarization states [9,11]. All of these effects have been studied experimentally as well as theoretically. Here we will concentrate on a further entangled property, the orbital angular momentum of the two generated photons [13,14]. The time entanglement arises from the energy conservation in the down-conversion process, which is expressed by the frequency matching condition. Similarly, the entanglement of the transverse position in the far field arises from the momentum conservation expressed by the phase-matching condition.

In this paper, we will show that the orbital angular momentum entanglement, a transverse property of the beam, follows also directly from the phase-matching condition and is related to the conservation of orbital angular momentum. Our approach differs from a recent theoretical paper [12] that dealt with the possible conservation of the combined spin and orbital angular momentum in relation to the susceptibility of the down-conversion crystal. The nonlinear electric susceptibility of the crystal determines the polarization properties of the down-converted photons. In the case of type I down-conversion, the polarization of the signal and the idler photons will be identical, its direction being determined by the polarization of the pump. In the case of type II down-conversion, the two down-converted photons have orthogonal polarizations. In specific setups, this can result in polarization entanglement in each pair of signal and idler photons. For each photon pair, be it generated in type I or type II

parametric down-conversion, phase-matching is fulfilled. Although the nature of the nonlinear susceptibility constrains the polarization of the three interacting waves, it in no way determines the orbital angular momentum of any of the beams. The orbital angular momentum is determined solely by the phase structure of each beam. Our analysis provides the theoretical background to a recent experiment, in which the conservation of the orbital angular momentum in parametric down-conversion has been observed for the first time [13,14].

While the spin angular momentum describes the intrinsic photon spin and corresponds to the optical polarization of light, the orbital angular momentum is associated with the transverse phase front of a light beam. Light with an azimuthal phase dependence  $\exp(il\varphi)$  carries a well-defined orbital angular momentum of  $l\hbar$  per photon [15]. The associated phase discontinuity produces an intensity null on the beam axis. Such light beams are conveniently described in terms of Laguerre-Gaussian modes, characterized by the mode indices  $l$  and  $p$ , where  $p+1$  gives the number of radial nodes, and  $2p+l$  the mode order  $N$ .

Laguerre-Gaussian beams can be generated by using holograms which have the form of distorted diffraction gratings with an  $l$ -pronged fork dislocation on the beam axis. The first-order diffracted beam then has  $l$  intertwined helical wavefronts. Alternatively, such holograms can be used in reverse to detect modes of a particular angular momentum number. In this configuration, if the number of dislocations in the hologram matches the angular momentum number of the incident beam, then the first-order diffracted beam has an on-axis intensity which can be detected. If, however, the number of forks does not match the number of dislocations, then no on-axis intensity results.

The correlation between Laguerre-Gaussian modes was studied in a recent down-conversion experiment [13,14]. For a pump beam with  $l_{\text{pump}}=0$ , nonvanishing coincidence count rates were measured for the detection of  $l_{\text{signal}}=2$  and  $l_{\text{idler}}=-2$ , whereas no significant coincidence rates were found, for example, for the detection of  $l_{\text{signal}}=\pm 2$  and  $l_{\text{idler}}=0$ . This suggests that the angular momentum is conserved in the down-conversion process, so that  $l_{\text{signal}}+l_{\text{idler}}=l_{\text{pump}}=0$ .

In the following, we derive the correlation between general transverse modes of the signal and idler photon. We then quantify these correlations for the special case of Laguerre-

Gaussian modes and show how these are related to the conservation of the orbital angular momentum.

Here we are concerned with the transverse-mode correlations between the signal and idler beams. Hence we describe the modes of the pump, signal, and idler by the normalized transverse mode functions  $\Phi_{0,1,2}(\mathbf{x})$ , where  $\mathbf{x}$  is a two-dimensional vector in the plane perpendicular to the propagation direction of the light; we work in the paraxial limit. Quantities and operators concerning the pump, signal, and idler are indicated by the subscripts 0, 1, and 2, respectively. For simplicity, we suppress the explicit beam propagation and assume frequency matching to be fulfilled.

We first determine the state of the light generated by a parametric down-conversion process [16,17]. In the Schrödinger picture, the two photons in the signal and the idler mode are created by applying the operator  $\hat{a}^\dagger(\mathbf{k}_1)\hat{a}^\dagger(\mathbf{k}_2)$  to the initial vacuum state  $|0\rangle$ , where  $\mathbf{k}_{1,2}$  is the transverse component of the signal and idler wave vector, respectively. Similarly,  $\mathbf{k}_0$  denotes the transverse component of the pump beam. We assume polarization states that are in agreement with the condition imposed by the nonlinear susceptibility of the crystal. For photons in such polarization states, phase-matching between the down-converted photons and the pump is satisfied. It can be described by a sinc function  $\Pi_{j=x,y} \text{sinc}[(\mathbf{k}_0 - \mathbf{k}_1 - \mathbf{k}_2)_j L_j / 2]$ , where  $L_j$  is the length of the crystal in the directions transverse to the beam propagation. For simplicity, we assume that the transverse dimension of the crystal is sufficiently large so that the phase-matching condition can be described by a two-dimensional delta function  $\delta^{(2)}(\mathbf{k}_0 - \mathbf{k}_1 - \mathbf{k}_2)$  and that all other modes are damped out [16,17]. Moreover, the fact that  $\mathbf{k}_0 - \mathbf{k}_1 - \mathbf{k}_2 = 0$  is a good approximation for fields carrying orbital angular momentum has already been experimentally verified in the frequency up-conversion of Laguerre-Gaussian modes [18]. While the  $\delta$  function constrains the sum of the transverse signal and idler wave vectors, their absolute difference  $|\mathbf{k}_1 - \mathbf{k}_2|$  cannot be arbitrarily large either. This is immediately apparent within the paraxial limit, the regime in which most down-conversion experiments are operating. More generally one can argue that large values of  $\mathbf{k}_1 - \mathbf{k}_2$  require large values of  $\mathbf{k}_1$  and/or  $\mathbf{k}_2$  and hence of the signal and idler frequencies  $\omega_1$  and  $\omega_2$ . Increasing  $|\mathbf{k}_1 - \mathbf{k}_2|$  to an arbitrarily large value, therefore, would lead to a violation of the frequency-matching condition  $\omega_0 = \omega_1 + \omega_2$  associated with energy conservation. Clearly, energy conservation requires  $|\mathbf{k}_1 - \mathbf{k}_2| \leq 2\pi/\lambda$ , where  $\lambda$  is the pump wavelength. We include this constraint in our analysis by means of the purely geometrical function  $\Delta(\mathbf{k}_1 - \mathbf{k}_2)$ , normalized such that  $\int d\mathbf{k} |\Delta(\mathbf{k})|^2 = 1$ . This function will be zero for large values of its argument so as to satisfy the requirement of energy conservation. In practice, other constraints including the sizes of apertures used and crystal geometry will prescribe the precise form of  $\Delta(\mathbf{k}_1 - \mathbf{k}_2)$ . We note that this function will result only in a scaling factor for the single and coincidence count rates. It cancels in the normalized count rates and plays no part in the derivation of orbital angular momentum conservation.

The two-photon wave function of the signal and idler then takes the form [19]

$$|\Psi\rangle = \int d\mathbf{k}_0 \int d\mathbf{k}_1 \int d\mathbf{k}_2 \Phi_0(\mathbf{k}_0) \hat{a}_2^\dagger(\mathbf{k}_2) \hat{a}_1^\dagger(\mathbf{k}_1) \times \Delta(\mathbf{k}_1 - \mathbf{k}_2) \delta^{(2)}(\mathbf{k}_0 - \mathbf{k}_1 - \mathbf{k}_2) |0\rangle. \quad (1)$$

Here

$$\Phi(\mathbf{k}_{0,1,2}) = \frac{1}{2\pi} \int d\mathbf{x} \Phi_{0,1,2}(\mathbf{x}_{0,1,2}) \exp(i\mathbf{k}_{0,1,2} \cdot \mathbf{x}_{0,1,2}) \quad (2)$$

denote the normalized mode functions in Fourier space. Similarly, the Fourier transformation of the creation operators is given by

$$\hat{a}_{1,2}^\dagger(\mathbf{k}_{1,2}) = \frac{1}{2\pi} \int d\mathbf{x} \hat{a}_{1,2}^\dagger(\mathbf{x}_{1,2}) \exp(-i\mathbf{k}_{1,2} \cdot \mathbf{x}_{1,2}). \quad (3)$$

Using these equations, we can write the two-photon wave function (1) in the position representation:

$$|\Psi\rangle = \int d\mathbf{x}_1 \int d\mathbf{x}_2 \Phi_0\left(\frac{\mathbf{x}_1 + \mathbf{x}_2}{2}\right) \times \Delta(\mathbf{x}_1 - \mathbf{x}_2) \hat{a}_1^\dagger(\mathbf{x}_1) \hat{a}_2^\dagger(\mathbf{x}_2) |0\rangle. \quad (4)$$

This is the normalized wave function of the combined system of the signal and idler generated by parametric down-conversion. It contains all necessary information about the outcome of single or coincidence measurements. The count rates of such measurements are proportional to the probabilities of detecting a photon of the signal or idler in the desired mode. In order to calculate these probabilities, we need to find the overlap of the two-photon state with the normalized one-photon state of the signal or idler,

$$|\Psi_{1,2}\rangle = \int d\mathbf{x}_{1,2} \Phi_{1,2}(\mathbf{x}_{1,2}) \hat{a}_{1,2}^\dagger(\mathbf{x}_{1,2}) |0\rangle, \quad (5)$$

associated with detecting a photon in the mode  $\Phi_{1,2}$ .

The coincidence probability for finding one photon in the signal mode  $\Phi_1$  and one photon in the idler mode  $\Phi_2$  is then given by

$$\begin{aligned} P(\Phi_1, \Phi_2) &= |\langle \Psi_2, \Psi_1 | \Psi \rangle|^2 \\ &= \left| \int d\mathbf{x}_1 \int d\mathbf{x}_2 \Phi_1^*(\mathbf{x}_1) \Phi_2^*(\mathbf{x}_2) \Phi_0 \right. \\ &\quad \left. \times \left(\frac{\mathbf{x}_1 + \mathbf{x}_2}{2}\right) \Delta(\mathbf{x}_1 - \mathbf{x}_2) \right|^2. \end{aligned} \quad (6)$$

If we average this expression over all possible signal modes, then we obtain the probability for finding a photon in the idler mode,

$$\begin{aligned}
P(\Phi_2) &= |\langle \Psi_2 | \Psi \rangle|^2 \\
&= \int d\mathbf{x}_1 \int d\mathbf{x}_2 \int d\mathbf{x}'_2 \Phi_2(\mathbf{x}'_2) \Phi_2^*(\mathbf{x}_2) \Phi_0^* \left( \frac{\mathbf{x}_1 + \mathbf{x}'_2}{2} \right) \\
&\quad \times \Phi_0 \left( \frac{\mathbf{x}_1 + \mathbf{x}_2}{2} \right) \Delta^*(\mathbf{x}_1 - \mathbf{x}'_2) \Delta(\mathbf{x}_1 - \mathbf{x}_2), \quad (7)
\end{aligned}$$

and a similar expression describes the probability of finding a single photon in the signal mode.

We recall that  $\Delta(\mathbf{k})$  is a very broad function that cuts out modes with large transverse wave vectors. The mode functions will therefore vary very little over the region where  $\Delta(\mathbf{x}_1 - \mathbf{x}_2)$ , the Fourier transform of  $\Delta(\mathbf{k})$ , does not vanish. Under this assumption, Eq. (6) and (7) can be written as

$$P(\Phi_1, \Phi_2) = \left| \int d\mathbf{y} \Delta(\mathbf{y}) \right|^2 \left| \int d\mathbf{x} \Phi_1^*(\mathbf{x}) \Phi_2^*(\mathbf{x}) \Phi_0(\mathbf{x}) \right|^2, \quad (8)$$

$$P(\Phi_2) = \left| \int d\mathbf{y} \Delta(\mathbf{y}) \right|^2 \int d\mathbf{x} |\Phi_2^*(\mathbf{x}) \Phi_0(\mathbf{x})|^2. \quad (9)$$

The factor  $|\int d\mathbf{y} \Delta(\mathbf{y})|^2$  will in general be very small and limit the count rates. This is because the down-converted photons are emitted into a wide spatial range.

The normalized coincidence probability, however, is independent of  $\Delta(\mathbf{y})$ :

$$\begin{aligned}
P(\Phi_1, \Phi_2)^N &= \frac{P(\Phi_1, \Phi_2)}{\sqrt{P(\Phi_1)P(\Phi_2)}} \\
&= \frac{\left| \int d\mathbf{x} \Phi_1^*(\mathbf{x}) \Phi_2^*(\mathbf{x}) \Phi_0(\mathbf{x}) \right|^2}{\sqrt{\int d\mathbf{x} |\Phi_2^*(\mathbf{x}) \Phi_0(\mathbf{x})|^2} \sqrt{\int d\mathbf{x} |\Phi_1^*(\mathbf{x}) \Phi_0(\mathbf{x})|^2}}. \quad (10)
\end{aligned}$$

This probability can take values between 0 and 1. It becomes 1 if signal and idler are perfectly correlated so that the detection of the signal in mode  $\Phi_1$  implies that the idler is in mode  $\Phi_2$ , and it vanishes if signal and idler are anticorrelated.

We now need to connect the idler mode function  $\Phi_0$  with the mode functions of the down-converted signal and idler  $\Phi_{1,2}$ . More precisely, we want to determine the idler mode for a given pump mode and detected signal mode. The state of the idler photon collapses into  $|\Psi_2\rangle = \langle \Psi_1 | \Psi \rangle$  if the signal photon was found to be in state  $|\Psi_1\rangle$ . We can calculate this state from Eqs. (4) and (5),

$$|\Psi_2\rangle = \int d\mathbf{y} \Delta(\mathbf{y}) \int d\mathbf{x}_2 \Phi_1^*(\mathbf{x}_2) \Phi_0(\mathbf{x}_2) \hat{a}^\dagger(\mathbf{x}_2) |0\rangle, \quad (11)$$

where we have evaluated the function  $\Delta(\mathbf{y})$  in the same way as previously. In comparison with Eq. (5), we find that the

mode function of the idler can be expressed as the product of the mode functions of the signal and the pump,

$$\Phi_2 = \left( \int d\mathbf{y} \Delta(\mathbf{y}) \right) \Phi_0 \Phi_1^*, \quad (12)$$

where the integral enforces the normalization of the idler mode. This may be interpreted “backwards” or retrodictively [20]: The measured mode function  $\Phi_2$  is “reflected” at the  $\chi^{(2)}$  crystal, where it interacts with the pump mode  $\Phi_0$  and is modified into the idler mode function.

So far our considerations have been valid for any transverse mode function, including Hermite or Laguerre-Gaussian modes. In the following, we will concentrate on Laguerre-Gaussian modes and specifically investigate the correlation of the orbital angular momentum between the signal and the idler. The normalized Laguerre-Gaussian modes in polar coordinates are given by

$$\begin{aligned}
\Phi_{p,l}(r, \varphi) &= \sqrt{\frac{2p!}{\pi(|l|+p)!}} \sqrt{\frac{1}{w} \left( \frac{r\sqrt{2}}{w} \right)^{|l|}} \\
&\quad \times L_p^{|l|} \left( \frac{2r^2}{w^2} \right) e^{-r^2/w^2} e^{-il\varphi}, \quad (13)
\end{aligned}$$

where the  $z$ -dependent phase was omitted and  $L_p^{|l|}$  denotes the associated Laguerre polynomial,

$$L_p^l = \sum_{m=0}^p (-1)^m C_{p-m}^{p+l} r^m / m!. \quad (14)$$

Laguerre-Gaussian modes with an integer orbital angular momentum of  $\hbar l$  per photon are orthonormal solutions of the paraxial wave equation. We note that these modes can be defined in the same way for fractional values of  $l$ . These fractional modes are still normalized, but form an overcomplete set. They can be written as sums of stable Laguerre-Gaussian modes with different integer  $l$ 's. As each of these modes has a different Gouy phase, the resulting beams with fractional  $l$ 's are unstable and do not maintain their amplitude distribution upon propagation. It has been suggested, however, that such beams can be prepared or detected by use of holograms or phaseplates [21] or by using nonlinear optical devices, such as the optical parametric oscillator [22].

By inserting the spatial mode functions  $\Phi_{p_{0,1,2}, l_{0,1,2}}$  in Eq. (12) and comparing the phase factors, we find that the orbital angular momentum of the idler is given by  $l_2 = l_0 - l_1$ . This signifies that the orbital angular momentum must be conserved,

$$l_0 = l_1 + l_2. \quad (15)$$

We want to stress that we have derived this equation solely from the phase-matching condition for Laguerre-Gaussian modes or other modes with the same azimuthal phase dependence. Our derivation is independent of the nature of the nonlinear susceptibility of the down-conversion crystal.

One example of the conservation of the orbital angular momentum can be seen in Fig. 1, where the mode profile of the idler mode function is shown as the product of the complex pump mode and the signal mode according to Eq. (12). Our derivation of Eq. (15) is valid for all modes that can be

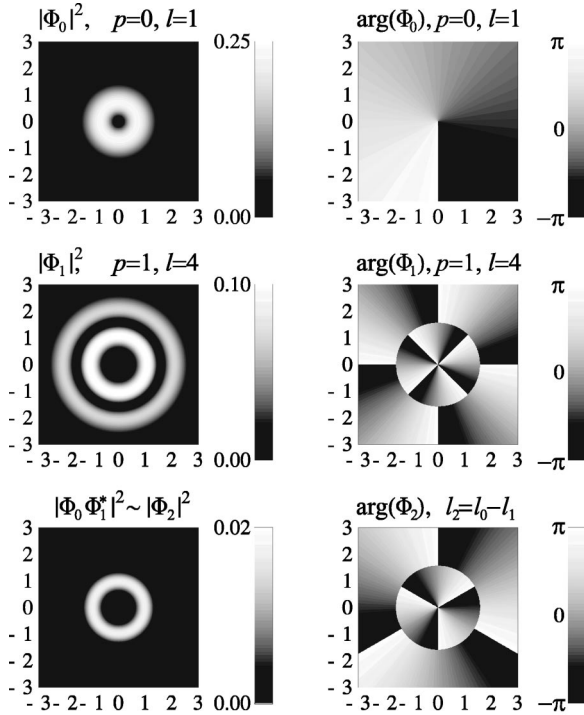


FIG. 1. Intensity  $|\Phi|^2$  and phase  $\arg(\Phi)$  of the pump, signal, and idler mode. If the pump and signal beams are prepared/measured in the indicated L-G modes, the idler collapses into a mode with an amplitude proportional to  $\Phi_0\Phi_1^*$ . The phase structure of the idler corresponds to  $l_2=l_0-l_1$  and an orbital angular momentum of  $3\hbar$ .

expressed in the form (13). We note that the conservation of orbital angular momentum can be fulfilled not only for integer quantities  $l_{0,1,2}$  but also for continuous values of the orbital angular momentum numbers.

Equation (15) is in agreement with the experimental observation of orbital angular momentum conservation reported in [13,14]. To our knowledge, this is the only relevant experiment at the single-photon level. Classical signal and idler beams consist of many photon pairs, for each of which the conservation  $l_0=l_1+l_2$  is satisfied. Both signal and idler beams will then exhibit modes with mixtures of various  $l$ 's rather than pure Laguerre-Gaussian modes [23]. These mixed signal and idler modes will still be correlated. However, unless we can observe each pair of photons, their correlation will be lost as there is no coherence between photons generated from different pump photons. This makes it very difficult to demonstrate the validity of Eq. (15) in the classical regime. In contrast to this, the orbital angular momentum of each photon created by a frequency-doubling process is uniquely determined as  $l_{2\omega}=2l_\omega$ , where  $l_\omega$  denotes the orbital angular momentum of the incoming photons. Consequently, the conservation of orbital angular momentum can be observed in classical up-conversion experiments [18].

The  $l$  conservation entangles the angular momentum modes of the signal and idler for a given pump mode. We set the waist of the idler equal to the waist of the signal,  $w_1=w_2=w$ , and denote the fraction of the signal and idler waist to the pump waist by  $W=w/w_0$ . By inserting the form

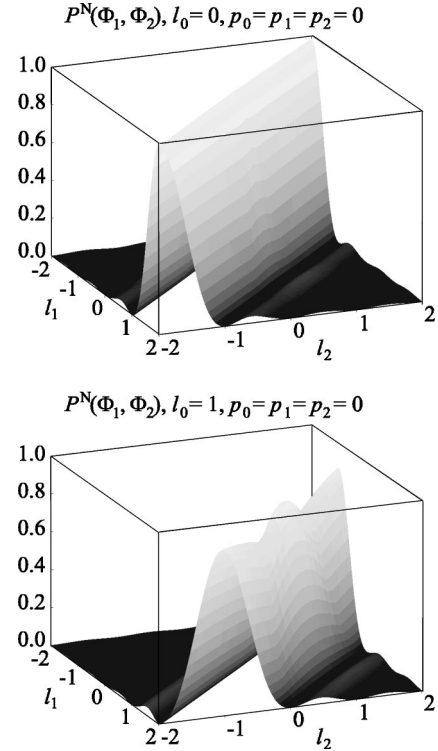


FIG. 2. The normalized coincidence probability  $P^N(\Phi_1, \Phi_2)$  for the orbital angular momenta of the signal and idler photons for  $l_0=0$  and 1. The ratio of idler and signal waists to that of the pump is  $W=0.4$ .

of Laguerre-Gaussian modes (13) into the normalized coincidence probability (10), we find

$$P^N(\Phi_1, \Phi_2) = \text{sinc}^2[(l_1 + l_2 - l_0)\pi] \frac{|R_{12}|^2}{\sqrt{R_2 R_1}}. \quad (16)$$

Here we have denoted

$$R_{12} = \int_0^\infty dr r^{(|l_1|+|l_2|+|l_0|)/2} e^{-r(1+W^2/2)} \times L_{p_1}^{|l_1|}(r) L_{p_1}^{|l_2|}(r) L_{p_0}^{|l_0|}(rW^2), \quad (17)$$

$$R_1 = \frac{(p_1 + |l_1|)!}{p_1!} \times \int_0^\infty dr r^{|l_2|+|l_0|} e^{-r(1+W^2)} [L_{p_1}^{|l_1|}(r)]^2 [L_{p_0}^{|l_0|}(rW^2)]^2, \quad (18)$$

and similarly for  $R_2$ . Figure 2 shows the normalized coincidence probability as a function of the continuous orbital angular momenta of the signal and idler photon.

The sinc function in Eq. (15) becomes maximal if the orbital angular momentum is conserved and vanishes if  $(l_0 - l_1 - l_2)$  is a nonzero integer. It is therefore most likely to detect a pair of signal and idler modes that conserve the pump angular momentum and it is impossible to find combinations of signal and idler modes that violate angular mo-



momentum conservation by an integer. Secondary maxima of the sinc function near half-integer values of  $(l_0 - l_1 - l_2)$  seem to imply that there is a violation of the conservation of orbital angular momentum. This is not the case, as the beams of fractional  $l$  may be expressed in terms of modes with integer  $l$ , some of which satisfy the conservation requirement. This is due to the fact that the fractional  $l$  modes are overcomplete. While this structure is determined by the phase dependence of the L-G modes, we find additional dips along the diagonals of maximum coincidence at  $l_1 + l_2 = l_0$ . These are related to the radial mode profile in Eq. (16) and again arise from the finite overlap of the fractional modes (12). There is no equivalent to this in polarization correlations. However, it should be stressed that this additional structure arises from the radial structure of the mode. If this radial structure is ignored, as in a detection process that measures only  $l$ , then this detailed structure disappears.

Compared with the spin angular momentum, orbital angular momentum offers a far richer structure. The spin angular momentum can only take values between  $-1$  and  $1$  for right and left circularly polarized light, respectively. The orbital angular momentum is in principle unlimited, and there exists an infinite number of Laguerre-Gaussian modes. While the spin angular momentum modes are defined in a two-dimensional Hilbert space, the orbital angular momentum modes occupy different Hilbert spaces depending on the mode order  $N = l + 2p$  with dimensionality  $N + 1$  [24].

Orbital angular momentum states with mode order  $N = 1$  are exactly analogous to spin angular momentum states. In each case they can be depicted on the Poincaré sphere [25]. Any two diametrically opposed points on the Poincaré sphere correspond to orthogonal states. For the polarization states these are left and right circular polarization, and horizontal and vertical linear polarization. For the orbital angular momentum states these are Laguerre-Gaussian modes with positive and negative phase, vertical and horizontal Hermite-Gaussian modes, or superpositions of such modes. It is well known [26] that maximum violation of Bell's inequality occurs between any two measurements made for polarization states separated by  $45^\circ$  on the Poincaré sphere. For orbital

angular momentum, states, we would therefore anticipate a maximum violation of Bell's inequality to be obtained for measurements of superpositions of Laguerre-Gaussian and Hermite-Gaussian modes of mode order 1 separated by  $45^\circ$  degree on the Poincaré sphere. For larger values of orbital angular momentum, this analogy breaks down due to the higher number of possible states. The quantum correlations, however, persist and offer the prospect of novel demonstrations and applications of entanglement.

Another approach has been proposed by Mair *et al.* [14], whereby a hologram displaced from its on-axis position no longer produces or detects a pure Laguerre-Gaussian mode but a complicated superposition of modes with differing indices. This situation can be modeled by a numerical evaluation of Eq. (10), which we will report elsewhere [27]. In general, the coincidence rate is maximized for hologram offsets, which result in mode combinations with high contributions by mode pairs which satisfy the conservation of orbital angular momentum (15), namely  $l_0 = l_1 + l_2$ .

In this paper, we have considered the correlation between Laguerre-Gaussian modes of the signal and idler with varying amounts of orbital angular momentum. The finite mode overlap between modes differing by a fractional number of  $l$  is to some extent reminiscent of the finite overlap between nonorthogonal polarization states, as they are used for testing Bell's inequality. This suggests the possibility of observing a violation of Bell's inequality for measurements of angular momentum states differing by fractional values of  $l$ . Such measurements may be possible with the use of holograms that impose a fractional change of the orbital angular momentum by means of a fractional change of the phase step.

We are grateful to Alois Mair for useful discussions and for providing us with invaluable information about his experiment on orbital angular momentum conservation. We would like to acknowledge the enthusiastic encouragement of the late Alan J. Duncan. This work was supported by the TMR program of the Commission of the European Union through the Quantum Structures Network and by the Leverhulme Trust.

- 
- [1] A. Einstein, B. Podolsky, and N. Rosen, *Phys. Rev.* **47**, 777 (1935).
- [2] J.S. Bell, *Physics* (Long Island City, N.Y.) **1**, 195 (1964); *Speakable and Unsayable in Quantum Mechanics* (Cambridge University Press, Cambridge, England, 1987).
- [3] A. Ekert, *Phys. Rev. Lett.* **67**, 661 (1991).
- [4] D. Bouwmeester, J.V. Pan, K. Mattle, M. Eible, H. Weinfurter, and A. Zeilinger, *Nature* (London) **390**, 575 (1997).
- [5] L.A. Lugiato and A. Gatti, *Phys. Rev. Lett.* **70**, 3868 (1993); A. Gatti and L.A. Lugiato, *Phys. Rev. A* **52**, 1675 (1995); A. Gatti, H. Wiedermann, L.A. Lugiato, I. Marzoli, G.-L. Oppo, and S.M. Barnett, *ibid.* **56**, 877 (1997).
- [6] T.B. Pittman, Y.H. Shih, D.B. Strekalov, and A.V. Sergienko, *Phys. Rev. A* **52**, R3429 (1995).
- [7] C.H. Monken, P.H. Souto Ribeiro, and S. Pádua, *Phys. Rev. A* **57**, 3123 (1998).
- [8] D.N. Klyshko and D.P. Krindach, *Pis'ma Zh. Éksp. Teor. Fiz.* **54**, 697 (1968) [*JETP Lett.* **17**, 371 (1968)].
- [9] P.G. Kwiat, K. Mattle, H. Weinfurter, A. Zeilinger, A.V. Sergienko, and Y. Shih, *Phys. Rev. Lett.* **75**, 4337 (1995).
- [10] J.G. Rarity, P.R. Tapster, E. Jakeman, T. Larchuk, R.A. Campos, M.C. Teich, and B.E.A. Saleh, *Phys. Rev. Lett.* **65**, 1348 (1990); Z.Y. Ou, X.Y. Zou, L.J. Wang, and L. Mandel, *Phys. Rev. A* **42**, 2957 (1990); Y.H. Shih and A.V. Sergienko, *Phys. Lett. A* **186**, 29 (1994).
- [11] Y.H. Shih, A.V. Sergienko, M.H. Rubin, T.E. Kiess, and C.O. Alley, *Phys. Rev. A* **50**, 23 (1994).
- [12] H.H. Arnaut and G.A. Barbosa, *Phys. Rev. Lett.* **85**, 286 (2000); E.R. Eliel *et al.*, *ibid.* **86**, 5208 (2001).
- [13] A. Mair and A. Zeilinger, *Vienna Circle Institute Yearbook 7/1999*, edited by A. Zeilinger *et al.* (Kluwer, Dordrecht, 1999).

- [14] A. E. Mair, Ph.D. thesis, Leopold Franzens Universität Innsbruck (2000) (in German); A. E. Mair, A. Vaziri, G. Weihs, and Anton Zeilinger, *Nature (London)* **412**, 313 (2001).
- [15] L. Allen, M.W. Beijersbergen, R.J.C. Spreeuw, and J.P. Woerdman, *Phys. Rev. A* **45**, 8185 (1992); M.W. Beijersbergen, L. Allen, H.E.L.O. van der Veen, and J. Woerdman, *Opt. Commun.* **96**, 123 (1992); L. Allen, M.J. Padgett, and M. Babiker, *Prog. Opt.* **39**, 291 (1999).
- [16] C.K. Hong and L. Mandel, *Phys. Rev. A* **31**, 2409 (1985).
- [17] See e.g., L. Mandel, and E. Wolf, *Optical Coherence and Quantum Optics* (Cambridge University Press, New York, 1995), p.1069f.
- [18] K. Dholakia, N.B. Simpson, M.J. Padgett, and L. Allen, *Phys. Rev. A* **54**, R3742 (1996); J. Courtial, K. Dholakia, L. Allen, and M.J. Padgett, *ibid.* **56**, 4193 (1997).
- [19] We note that, if we wanted to include polarization properties in our calculation, we would need to consider the nonlinear susceptibility tensor in Eq. (1).
- [20] D.T. Pegg and S.M. Barnett, *J. Opt. B: Quantum Semi-Classical Opt.* **1**, 442 (1999), and references therein.
- [21] M.W. Beijersbergen, R.P.C. Coerwinkel, M. Kristensen, and J.P. Woerdman, *Opt. Commun.* **112**, 321 (1994).
- [22] G.-L. Oppo, A.J. Scroggie, and W.J. Firth, *Phys. Rev. E* **63**, 066209 (2001).
- [23] J. Arlt, K. Dholakia, L. Allen, and M.J. Padgett, *Phys. Rev. A* **59**, 3950 (1999).
- [24] L. Allen, J. Courtial, and M.J. Padgett, *Phys. Rev. E* **60**, 7497 (1999).
- [25] M.J. Padgett and J. Courtial, *Opt. Lett.* **24**, 430 (1999).
- [26] See, e.g., A.J. Duncan, *Progress in Atomic Spectroscopy* (Plenum Press, New York, 1987), pp. 477–505.
- [27] M.J. Padgett, J. Courtial, L. Allen, S. Franke-Arnold, and S.M. Barnett, *J. Mod. Opt.* (to be published).